Hsp90 of *E. coli* modulates assembly of FtsZ, the bacterial tubulin homolog

Anuradha Balasubramanian[a,1], Monica Markovski[a,2], Joel R. Hoskins[a], Shannon M. Doyle[a,3], and Sue Wickner[a,3]

[a]Laboratory of Molecular Biology, National Cancer Institute, National Institutes of Health, Bethesda, MD 20892

Heat shock protein 90 (Hsp90) is a highly conserved molecular chaperone involved in ATP-dependent client protein remodeling and activation. It also functions as a protein holdase, binding and stabilizing clients in an ATP-independent process. Hsp90 remodels over 300 client proteins and is essential for cell survival in eukaryotes. In bacteria, Hsp90 is a highly abundant protein, although very few clients have been identified and it is not essential for growth in many bacterial species. We previously demonstrated that in *Escherichia coli*, Hsp90 causes cell filamentation when expressed at high levels. Here, we have explored the cause of filamentation and identified a potentially important client of *E. coli* Hsp90 (Hsp90$_{Ec}$), FtsZ. We observed that FtsZ, a bacterial tubulin homolog essential for cell division, fails to assemble into FtsZ rings (divisomes) in cells overexpressing Hsp90$_{Ec}$. Additionally, Hsp90$_{Ec}$ interacts with FtsZ and inhibits polymerization of FtsZ in vitro, in an ATP-independent holding reaction. The FtsZ–Hsp90$_{Ec}$ interaction involves residues in the client-binding region of Hsp90$_{Ec}$ and in the C-terminal tail of FtsZ, where many cell-division proteins and regulators interact. We observed that *E. coli* deleted for the Hsp90$_{Ec}$ gene *htpG* turn over FtsZ more rapidly than wild-type cells. Additionally, the length of Δ*htpG* cells is reduced compared to wild-type cells. Altogether, these results suggest that Hsp90$_{Ec}$ is a modulator of cell division, and imply that the polypeptide-holding function of Hsp90 may be a biologically important chaperone activity.

HtpG | substrate | holdase | ClpXP

Heat shock protein 90 (Hsp90) is a highly conserved molecular chaperone involved in protein homeostasis. In eukaryotes, Hsp90 is essential and is involved in remodeling, activating, and stabilizing numerous client proteins (1–3). *Escherichia coli* Hsp90, encoded by *htpG* and referred to as Hsp90$_{Ec}$, is abundant under normal nonstress conditions, and its level increases during stress conditions (4, 5). Although Hsp90$_{Ec}$ is not essential, *E. coli* strains lacking Hsp90$_{Ec}$, compared with wild type, have a slight growth defect at elevated temperatures (4, 6), have increased levels of aggregated proteins following heat stress (7), exhibit swarming defects (8), have decreased ability to form biofilms at elevated temperatures (9), and lose adaptive immunity conferred by the CRISPR system (10).

Hsp90 chaperones have been shown to function as dimers, with each monomer composed of three domains: an N-terminal ATP-binding domain, a middle domain involved in binding Hsp70 and interacting with client proteins, and a C-terminal domain involved in client binding and dimerization (2, 3, 11–13). Structural and biochemical studies have demonstrated that ATP binding and hydrolysis by Hsp90 trigger large conformational changes that are coupled to client binding, remodeling, and release in a process that results in reactivation of inactive proteins (3, 11, 13, 14). In eukaryotes, protein remodeling by Hsp90 requires cochaperones, of which there are more than 20 (3, 15). Moreover, the Hsp70 chaperone and its two cochaperones, a J-domain protein and a nucleotide exchange factor, are also required for some eukaryotic Hsp90-remodeling reactions (2, 3). In contrast, bacterial homologs of eukaryotic Hsp90 cochaperones have not been identified, and the combination of bacterial Hsp90 and the bacterial Hsp70 system is sufficient to reactivate clients in vitro (11, 16). In addition

to remodeling proteins, eukaryotic and prokaryotic Hsp90s bind polypeptides and prevent aggregation (17–20). This activity is independent of cochaperones and ATP hydrolysis (12, 17, 19–22).

We previously showed that expression of Hsp90$_{Ec}$ from an inducible plasmid in *E. coli* causes a block in cell division and results in filamentous cells (22). *E. coli* cell division is a complex and highly regulated process of (*i*) DNA replication, (*ii*) chromosome segregation, (*iii*) assembly of the divisome at midcell, (*iv*) constriction of the divisome, and (*v*) separation of the two daughter cells (23–27). Divisome assembly and constriction require a precise balance of more than a dozen proteins and is regulated by numerous others. The central and most abundant component is FtsZ, which assembles into a membrane-associated cytokinetic ring, the FtsZ ring, at midcell and recruits additional divisome components (25–27). FtsZ is a structural homolog of eukaryotic tubulin and, like tubulin, it polymerizes in the presence of GTP (28–30). The polymers are dynamic, and subunits are rapidly exchanged (31, 32). The FtsZ ring is composed of short, discontinuous polymers that, with the help of other cell-division components, are stabilized by lateral interactions and tethered to the membrane. FtsZ polymer dynamics are regulated by both positive and negative regulator proteins. In *E. coli*, proteins that promote FtsZ polymerization and/or bundling include the positive regulators FtsA, ZipA, ZapA, ZapC, and ZapD; conversely, negative regulators MinC, SlmA, SulA, Pgm, and ClpXP promote polymer disassembly (33–35).

Significance

Hsp90 is a molecular chaperone that participates in protein remodeling and activation. We previously demonstrated that Hsp90 causes cell filamentation when highly expressed in *E. coli*. Here we show that cells filament due to overexpression of Hsp90$_{Ec}$ because FtsZ, a bacterial tubulin homolog essential for cell division, fails to assemble into FtsZ rings. In vitro, Hsp90$_{Ec}$ interacts with FtsZ and inhibits FtsZ polymerization. Moreover, *E. coli* deleted for the Hsp90$_{Ec}$ gene, *htpG*, turn over FtsZ more rapidly than wild-type cells, and the length of Δ*htpG* cells is reduced compared to wild-type cells. Altogether, these results suggest that Hsp90$_{Ec}$ is a modulator of cell division, and imply that the polypeptide-holding function of Hsp90 may be a biologically important chaperone activity.
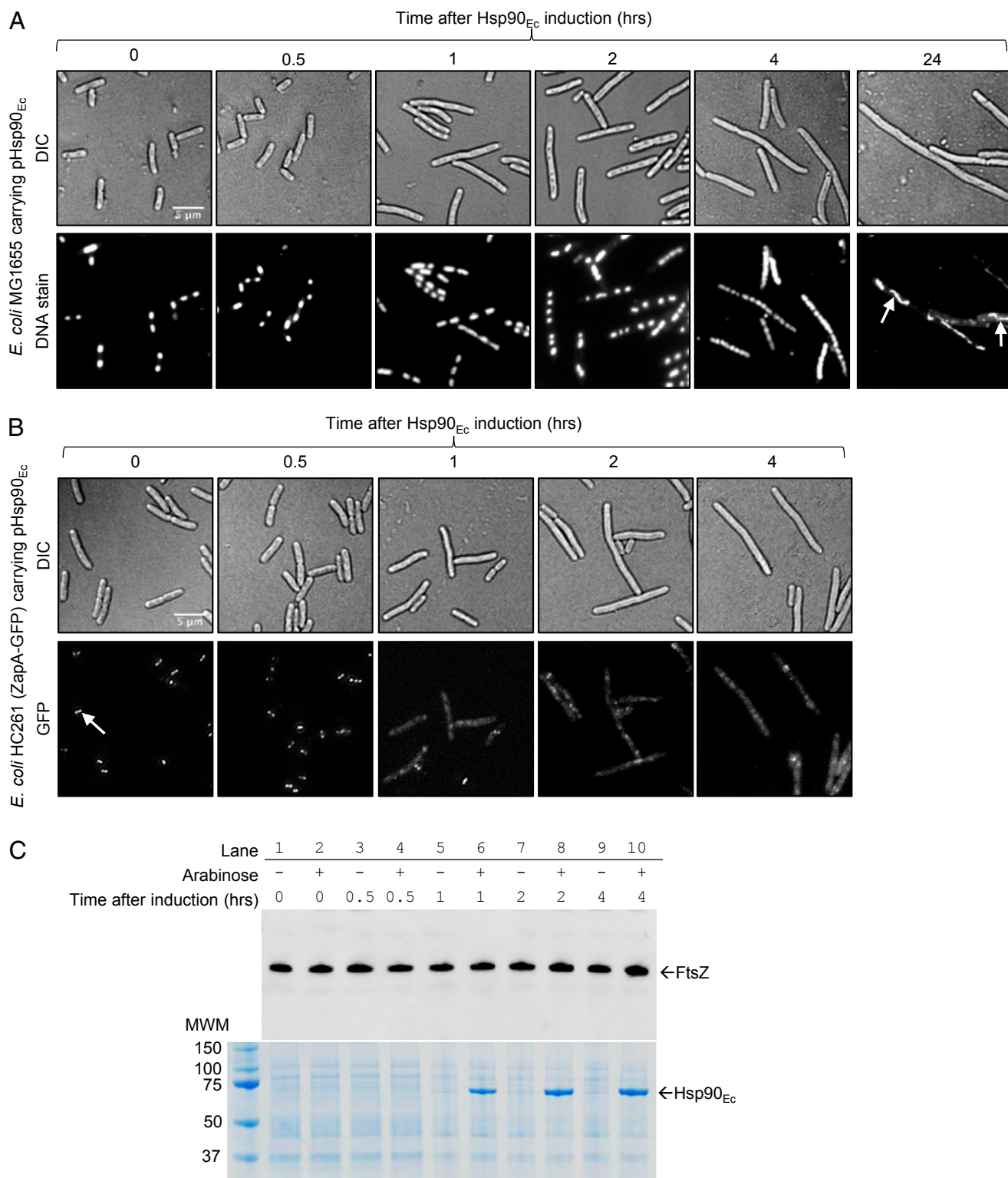
BIOCHEMISTRY

www.manaraa.com

Fig. 1. Overexpression of Hsp90$_{Ec}$ causes cell filamentation and inhibits FtsZ-ring formation. (*A*) *E. coli* MG1655 carrying pHsp90$_{Ec}$ was grown in the presence of inducer (0.2% arabinose) for the times indicated. Cells were stained with Syto 9, a nucleoid stain, and analyzed by DIC and fluorescence microscopy as described in *Materials and Methods*. Arrows (24-h panel) indicate unsegregated nucleoids. (*B*) *E. coli* HC261, expressing ZapA-GFP from the chromosome and carrying pHsp90$_{Ec}$, was grown with inducer (0.2% arabinose) for the times indicated and samples were analyzed by DIC and fluorescence microscopy. The arrow (0-h panel) indicates a fluorescent FtsZ ring. (*C*) *E. coli* MG1655 carrying pHsp90$_{Ec}$ was grown ±inducer (0.2% arabinose). Samples were collected at the indicated times and analyzed by SDS/PAGE followed by immunoblotting with anti-FtsZ antibody (*Top*) or Coomassie staining (*Bottom*) as described in *Materials and Methods*. (Scale bars, 5 μm.) Experiments are representative of three replicates.

Balasubramanian et al.

www.manaraa.com

Here, we explored the cause of the filamentous phenotype of cells overexpressing $Hsp90_{Ec}$ from a plasmid carrying *htpG* under the control of an inducible promoter. Our results show that FtsZ does not assemble into FtsZ rings in cells overexpressing $Hsp90_{Ec}$. Moreover, $Hsp90_{Ec}$ interacts with FtsZ and inhibits FtsZ polymerization in vitro. Together, our results suggest that $Hsp90_{Ec}$ modulates cell division through its ATP hydrolysis-independent holdase activity.

Results

FtsZ Rings Do Not Assemble When $Hsp90_{Ec}$ Is Highly Expressed. To gain insight into the in vivo activities of *E. coli* Hsp90, referred to as $Hsp90_{Ec}$, we explored a phenotype associated with $Hsp90_{Ec}$ overexpression. Our previous work showed that rod-shaped wild-type *E. coli* cells become filamentous when $Hsp90_{Ec}$ is overexpressed from a plasmid, $pHsp90_{Ec}$ (*SI Appendix*, Table S1) (22). A closer examination showed that short filamentous cells, two- to fourfold longer than normal cells, first appeared ∼1 h after $Hsp90_{Ec}$ induction (Fig. 1*A*). At this time, the level of $Hsp90_{Ec}$ was ∼100-fold higher than in uninduced cells, as determined by quantification of Western blots (*SI Appendix*, Fig. S1 *A* and *B*). The filaments continued to increase in length until growth ceased in stationary phase (Fig. 1*A*). Points of membrane invagination were not seen in the growing filaments, suggesting that cell division was blocked before septum constriction.

To investigate how overexpression of $Hsp90_{Ec}$ arrests cell division, we monitored the appearance of nucleoids by DNA staining to determine if the filamentous cells overproducing $Hsp90_{Ec}$ were able to replicate DNA and segregate nucleoids. We observed that the nucleoids were discrete and evenly spaced throughout the filaments for at least 2 h after induction, when the cells were clearly elongating and becoming filamentous (Fig. 1*A*). These observations suggest that during the first several hours of $Hsp90_{Ec}$ overexpression, cells can replicate and segregate their nucleoids, although cell division is defective. At the 24-h postinduction time point, abnormal nucleoids that appeared to have failed to segregate were prevalent, suggesting additional defects in chromosome replication and segregation do occur at later time points (Fig. 1*A*).

Since FtsZ-ring formation is the step in cell division that immediately follows nucleoid segregation, we tested if cells form FtsZ rings after $Hsp90_{Ec}$ induction. We visualized FtsZ rings in living cells using a previously described assay that involves ZapA-GFP as a proxy for FtsZ (36, 37). This assay was used because FtsZ-GFP is unable to complement an *ftsZ* null mutant, which indicates that FtsZ-GFP is not fully functional (38). In contrast to FtsZ, ZapA is a nonessential division protein that is known to associate with the FtsZ ring (37). Moreover, cells expressing ZapA-GFP grow normally and ZapA-GFP associates with the FtsZ ring, allowing visualization of the FtsZ ring by fluorescence microscopy (37). We transformed $pHsp90_{Ec}$ into cells expressing ZapA-GFP from a gene fusion in the chromosome, induced $Hsp90_{Ec}$ expression, and examined the cells by fluorescence microscopy (Fig. 1*B*). In uninduced cells, ZapA-GFP was located at midcell (Fig. 1*B*, 0 h and *SI Appendix*, Fig. S1*C*), as previously observed for cells not carrying an additional plasmid (37), indicating that FtsZ rings were also localized at midcell. After 1 or more hours of $Hsp90_{Ec}$ induction, only a few FtsZ rings were observed per filamentous cell (Fig. 1*B*). We also observed FtsZ rings directly by fluorescent immunostaining of FtsZ in fixed cells (*SI Appendix*, Fig. S1*D*). FtsZ rings were less prevalent after 1 h of $Hsp90_{Ec}$ overexpression compared with the uninduced control, and were not detectable after 2 or 4 h of induction (*SI Appendix*, Fig. S1*D*). Together, these observations indicate that overexpression of $Hsp90_{Ec}$ blocks FtsZ-ring formation.

To test if the filamentous phenotype associated with $Hsp90_{Ec}$ overexpression could be reversed, we induced cells carrying $pHsp90_{Ec}$ and expressing ZapA-GFP from the chromosome for

6 h and then removed the inducer by washing the cells and diluting them in fresh media. We observed that the cells resumed growth (*SI Appendix*, Fig. S2*A*) and by 2 h postdilution the filaments became shorter and distinct FtsZ rings reappeared, as monitored by fluorescence microscopy of the cells (*SI Appendix*, Fig. S2*B*). At 3 h postdilution, the recovering cells were indistinguishable from uninduced cells (*SI Appendix*, Fig. S2*B*). These results suggest that high levels of $Hsp90_{Ec}$ arrest cell division but do not lead to cell death during the first 6 h of overexpression.

Cellular Levels of FtsZ Are Not Affected by Overexpression of $Hsp90_{Ec}$. To determine if overexpression of $Hsp90_{Ec}$ affects the cellular level of FtsZ, we induced $Hsp90_{Ec}$ in cells carrying $pHsp90_{Ec}$ and measured the levels of FtsZ. We observed that there was no detectable change in the steady-state level of FtsZ during 4 h of induction as determined by SDS/PAGE and Western blot analysis (Fig. 1*C*). In the same cell culture, the level of $Hsp90_{Ec}$ increased greatly in the first hour of induction compared with uninduced cells, as seen by Coomassie staining (Fig. 1*C*) and quantified by Western blot analysis (*SI Appendix*, Fig. S1 *A* and *B*), and then remained high. Thus, although FtsZ is not localized to midcell and cells do not divide, the FtsZ level remains constant in cells expressing high levels of $Hsp90_{Ec}$. These results indicate that $Hsp90_{Ec}$ does not inhibit FtsZ synthesis or facilitate FtsZ degradation but instead $Hsp90_{Ec}$ appears to inhibit FtsZ activity.

Next, we monitored the levels of FtsZ and $Hsp90_{Ec}$ in cells recovering from $Hsp90_{Ec}$ overexpression-induced filamentation (*SI Appendix*, Fig. S2 *A* and *B*). Following removal of the inducer, the FtsZ level in the cells, as monitored by Western blot analysis, remained roughly constant throughout the course of the experiment even as the FtsZ rings reappeared (*SI Appendix*, Fig. S2 *B* and *C*). However, the level of $Hsp90_{Ec}$ decreased significantly with time after removal of the inducer (*SI Appendix*, Fig. S2*C*). These results suggest that overexpressing $Hsp90_{Ec}$ does not kill cells and that inhibition of division is relieved when the ratio of $Hsp90_{Ec}$ to FtsZ decreases, which likely happens by dilution as the cells grow in the absence of inducer.

FtsZ Overexpression Suppresses the Filamentous Phenotype of $Hsp90_{Ec}$ Overexpression. The observation that high levels of $Hsp90_{Ec}$ do not affect the FtsZ level is consistent with the idea that $Hsp90_{Ec}$ binds FtsZ and prevents FtsZ-ring assembly. This hypothesis is attractive because Hsp90 is known to bind stoichiometrically to nonnative and unfolded proteins and prevent aggregation in vitro, using its ATP hydrolysis-independent holding activity (17–21). A mechanism with $Hsp90_{Ec}$ holding FtsZ is further supported by our observation that overexpression of $Hsp90_{Ec}$-E34A, a mutant defective in ATP hydrolysis, causes cell filamentation indistinguishable from that caused by overexpression of wild-type $Hsp90_{Ec}$ (22).

The hypothesis that high levels of $Hsp90_{Ec}$ prevent cell division by sequestering FtsZ protomers predicts that excess FtsZ expressed from a plasmid will prevent the cell-division arrest caused by overexpression of $Hsp90_{Ec}$ from a plasmid. To test this possibility, we used a previously characterized plasmid, pZAQ (39, 40), that expresses FtsZ, FtsA, and FtsQ under the control of the native, constitutive promoter. FtsA and FtsQ, like FtsZ, are essential divisome components (26, 33). pZAQ was cotransformed into a strain expressing $Hsp90_{Ec}$ from a compatible plasmid, pBAD33 (called $p_{33}Hsp90_{Ec}$), under the control of the arabinose promoter. As previously seen, cells expressing pZAQ were rod-shaped with a reduced cell length compared with wild-type cells (Fig. 2*A*) (39). Cells carrying $p_{33}Hsp90_{Ec}$ and incubated for 4 h with the inducer, arabinose, exhibited a filamentous phenotype (Fig. 2*A*). When cells carrying both pZAQ and $p_{33}Hsp90_{Ec}$ were incubated with arabinose for 4 h, the cells appeared as rods, indistinguishable from cells expressing pZAQ alone (Fig. 2*A*). FtsZ was expressed at approximately twofold higher levels in cells expressing pZAQ and $p_{33}Hsp90_{Ec}$, compared with cells expressing $p_{33}Hsp90_{Ec}$ alone
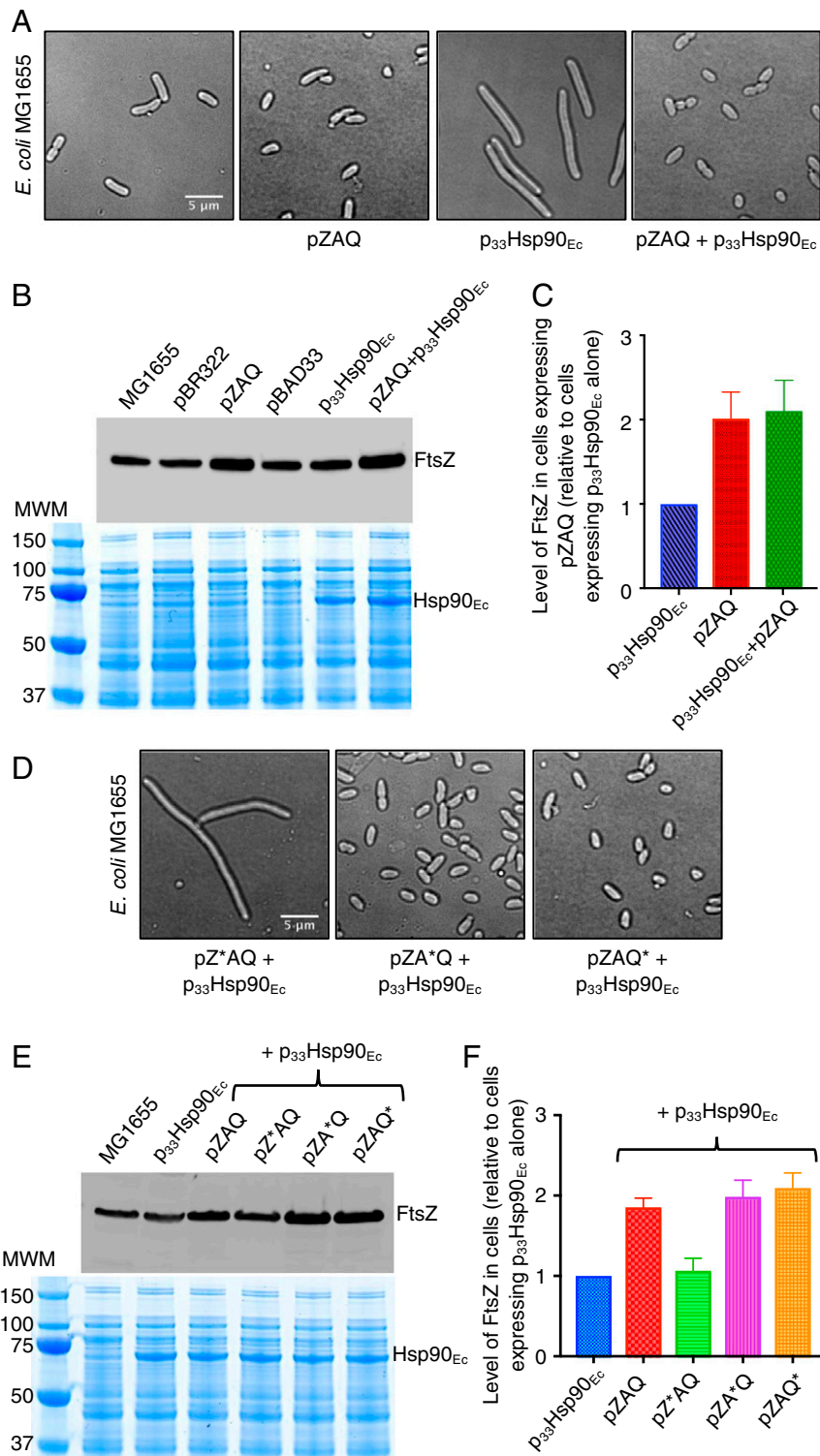
BIOCHEMISTRY

www.manaraa.com

Fig. 2. FtsZ overexpression suppresses the filamentous phenotype of cells expressing high levels of Hsp90$_{Ec}$. (*A*) *E. coli* MG1655 carrying pZAQ, p$_{33}$Hsp90$_{Ec}$, or both pZAQ and p$_{33}$Hsp90$_{Ec}$ were grown for 4 h at 37 °C in the presence of 0.2% arabinose to induce Hsp90$_{Ec}$ and DIC images were acquired. (*B*) Cell samples from cultures grown as described in *A* and normalized to OD$_{600}$ were analyzed by SDS/PAGE followed by immunoblotting with anti-FtsZ antibody as described in *Materials and Methods* (*Top*) or Coomassie staining (*Bottom*). (*C*) Quantification of FtsZ immunoblots shown in *B*. Data from three replicates were normalized to the FtsZ level in induced cells carrying p$_{33}$Hsp90$_{Ec}$ and are presented ±SD. (*D*) *E. coli* MG1655 carrying p$_{33}$Hsp90$_{Ec}$ and pZ*AQ, pZA*Q, or pZAQ* were grown in the presence of 0.2% arabinose for 4 h at 37 °C and DIC images were acquired. (*E*) Cell samples from cultures grown as described in *D* and normalized to OD$_{600}$ were analyzed by SDS/PAGE followed by immunoblotting with anti-FtsZ antibody (*Top*) or Coomassie staining (*Bottom*). (*F*) Quantification of FtsZ immunoblots shown in *E*. Data from three replicates were normalized to the FtsZ level in induced cells carrying p$_{33}$Hsp90$_{Ec}$ and are presented as mean ± SD. (Scale bars, 5 μm.) In *D*–*F*, * indicates the gene that contains a frameshift mutation: *ftsZ*, *ftsA*, or *ftsQ*. Experiments in *A*, *B*, *D*, and *E* are representative of three replicates.

Balasubramanian et al.

www.manaraa.com

(Fig. 2 *B* and *C*). In control experiments, we observed that FtsZ was expressed at similar levels in cells carrying no plasmid, p$_{33}$Hsp90$_{Ec}$, pBR322, or pBAD33 (Fig. 2 *B* and *C*). Cells carrying the p$_{33}$Hsp90$_{Ec}$ plasmid expressed Hsp90$_{Ec}$ at ~30-fold higher levels when induced, compared with cells carrying the vector only (Fig. 2*B* and *SI Appendix*, Fig. S2 *D* and *E*). Thus, the filamentous phenotype of cells overexpressing Hsp90$_{Ec}$ is suppressed by expression of additional FtsZ, FtsA, and FtsQ.

To determine if FtsZ alone was sufficient to compensate for Hsp90$_{Ec}$ overexpression, frameshift mutations were introduced into each of the three genes *ftsZ*, *ftsA*, or *ftsQ* separately in the pZAQ plasmid as previously described (39). The resulting plasmids, pZ*AQ, pZA*Q, and pZAQ* (* indicates the gene with the mutation), were cotransformed with p$_{33}$Hsp90$_{Ec}$ into *E. coli* cells. After incubation with arabinose for 4 h, the cells expressing Hsp90$_{Ec}$ in addition to Z*AQ were filamentous; cells expressing Hsp90$_{Ec}$ and either ZA*Q or ZAQ* were small and rod-shaped (Fig. 2*D*). Consistent with the phenotype, cells carrying p$_{33}$Hsp90$_{Ec}$ and induced with arabinose in the absence or presence of pZ*AQ only produced ~50% the amount of FtsZ as cells expressing p$_{33}$Hsp90$_{Ec}$ and pZA*Q, pZAQ*, or pZAQ (Fig. 2 *E* and *F*). When induced with arabinose, Hsp90$_{Ec}$ was expressed at higher levels in cells carrying p$_{33}$Hsp90$_{Ec}$ alone or in combination with pZAQ, pZ*AQ, pZA*Q, or pZAQ*, compared with cells not carrying p$_{33}$Hsp90$_{Ec}$ (Fig. 2*E* and *SI Appendix*, Fig. S2 *D* and *E*). These results indicate that an increase in FtsZ levels can prevent cell filamentation caused by Hsp90$_{Ec}$ overexpression, and suggest that Hsp90$_{Ec}$ overexpression prevents FtsZ from functioning in cell division.

Consistent with the interpretation that Hsp90$_{Ec}$ overexpression inhibits the activity of FtsZ directly and not indirectly by stabilizing a negative regulator of FtsZ, we observed that overexpressed Hsp90$_{Ec}$ acts independent of several FtsZ negative regulators. Since it was known from previous work that cells overexpressing Hsp90$_{Ec}$ from pHsp90$_{Ec}$ are sensitive to 1% SDS (22), we monitored the SDS sensitivity of cells carrying a deletion in an FtsZ negative regulator gene and overexpressing Hsp90$_{Ec}$ from a plasmid. When Hsp90$_{Ec}$ was overexpressed in a Δ*minC*, Δ*slmA*, Δ*sulA*, or Δ*clpX* strain, we observed that the cells were sensitive to 1% SDS, as was the wild-type strain (*SI Appendix*, Fig. S3 *A–C*). As seen previously, cells not overexpressing Hsp90$_{Ec}$ were resistant to SDS (22). Strains carrying a deletion in another negative regulator, *Pgm*, were previously shown to be sensitive to 1% SDS (41), and were not tested in this assay. However, overexpression of Hsp90$_{Ec}$ in Δ*pgm* cells resulted in filamentation as observed by microscopy (*SI Appendix*, Fig. S3*D*). Together, these observations suggest that Hsp90$_{Ec}$ acts independent of these negative cell-division regulators.

FtsZ Is Less Stable in an *E. coli* Δ*htpG* Strain Compared with the Wild-Type Strain. Previous results suggested that bacterial Hsp90s, including Hsp90$_{Ec}$, protect some clients from degradation (10, 42, 43). Moreover, *E. coli* FtsZ is known to be degraded in vivo and in vitro by the ClpXP protease (44). To test if Hsp90$_{Ec}$ is able to protect FtsZ from degradation, we monitored FtsZ degradation in both wild-type MG1655 and Δ*htpG* cells, after blocking protein synthesis with spectinomycin. As previously observed (44), FtsZ is a long-lived protein; with the strain and conditions used in this study, the half-life of FtsZ in wild type was ~219 min (Fig. 3 *A* and *B*). In contrast, FtsZ in the Δ*htpG* strain was degraded faster than in the wild-type strain, with a half-life of ~132 min (Figs. 3 *A* and *B* and *SI Appendix*, Fig. S4*A*). These results suggest that Hsp90$_{Ec}$ protects FtsZ from degradation in vivo.

We also tested if Hsp90$_{Ec}$ was able to protect FtsZ from degradation by ClpXP in vitro. We found that FtsZ degradation by ClpXP was inhibited ~45% by the presence of an equimolar concentration of Hsp90$_{Ec}$ (Fig. 3*C*). These results suggest that Hsp90$_{Ec}$ is able to protect FtsZ from degradation by ClpXP.

The Length of *E. coli* Δ*htpG* Cells Is Reduced Compared to Wild-Type Cells. To explore the possible physiological role of Hsp90$_{Ec}$ in *E. coli* cell division, we compared the appearance of Δ*htpG* and wild-type cells by microscopy. Surprisingly, the Δ*htpG* cells exhibited reduced cell length compared to wild-type cells (Fig. 3*D*), although the two strains grew at similar rates as monitored by cell density (OD$_{600}$) (*SI Appendix*, Fig. S4*B*). Cell-length determination showed that Δ*htpG* cells were ~25% shorter than wild-type cells with a mean length of 2.74 ± 0.47 μm for Δ*htpG* cells compared with 3.62 ± 0.80 μm for wild-type cells (Fig. 3*E*). The difference in cell length was observed both in log-phase cells (Fig. 3 *D* and *E*) and in early stationary-phase cells (*SI Appendix*, Fig. S4 *C* and *D*). These results suggest the possibility that the loss of Hsp90$_{Ec}$ holdase activity in Δ*htpG* cells leads to an increase in available FtsZ and this increase in functional FtsZ results in the small-cell phenotype. This interpretation is consistent with previous reports that cells expressing increased levels of FtsZ divide prematurely and are smaller (40, 45). However, the possibility that the small-cell phenotype may also be due to any number of metabolic changes resulting from the lack of Hsp90$_{Ec}$ has not been explored.

Hsp90$_{Ec}$ Inhibits FtsZ Polymerization In Vitro. Our in vivo observations showing that Hsp90$_{Ec}$ prevents FtsZ-ring formation without significantly decreasing the cellular level of FtsZ prompted us to test the possibility that Hsp90$_{Ec}$ interacts with unassembled FtsZ and inhibits FtsZ polymerization in vitro. We used fluorescence microscopy to visualize the effect of Hsp90$_{Ec}$ on the polymerization of FtsZ labeled with Alexa Fluor 488 (FtsZ$_{AF488}$). In control experiments, FtsZ$_{AF488}$ could be seen as fibers and bundles in the presence of GTP but not in the absence, as previously observed (30, 44) (Fig. 4*A*, *1* and *2*). In contrast, when FtsZ$_{AF488}$ was incubated with Hsp90$_{Ec}$, in a ratio of 1:0.5, before the addition of GTP, FtsZ$_{AF488}$ fibers were not detected, although some small aggregates were observed (Fig. 4*A*, *3*). Addition of Hsp90$_{Ec}$ had no detectable effect on the quantity or appearance of FtsZ$_{AF488}$ fibers when it was added after FtsZ$_{AF488}$ polymerization was initiated with GTP (Fig. 4*A*, *4*). ATP was not included in these experiments, indicating that prevention of polymerization of FtsZ$_{AF488}$ did not require ATP hydrolysis by Hsp90$_{Ec}$. Addition of ATP with GTP had no significant effect on the prevention of FtsZ$_{AF488}$ polymerization (*SI Appendix*, Fig. S4*E*). Additionally, the ATP hydrolysis-defective Hsp90$_{Ec}$ mutant E34A (16, 46) was able to prevent FtsZ$_{AF488}$ polymerization (Fig. 4*A*, *5*). This observation is consistent with the previous observation that Hsp90$_{Ec}$-E34A overexpression in cells caused cell filamentation like wild-type Hsp90$_{Ec}$ (22). These results suggest that the holdase function of Hsp90$_{Ec}$ is involved in the prevention of FtsZ polymerization rather than the ATP-dependent chaperone activity of Hsp90$_{Ec}$.

The localization of Hsp90$_{Ec}$ was also followed in these polymerization experiments using fluorescently labeled Hsp90$_{Ec}$ (Hsp90$_{Ec-AF594}$). We observed that Hsp90$_{Ec-AF594}$ associated with preformed FtsZ polymers when added after FtsZ and GTP (Fig. 4*B*, *1*). However, when Hsp90$_{Ec-AF594}$ was added to FtsZ before GTP induced polymerization, no large fibers were detected but some small aggregates were observed (Fig. 4*B*, *2*). In a control experiment, a few small aggregates were visible when Hsp90$_{Ec-AF594}$ was incubated with GTP in the absence of FtsZ (Fig. 4*B*, *3*). Together, these results suggest Hsp90$_{Ec}$ interacts with unassembled FtsZ and inhibits polymerization but can also interact with assembled FtsZ polymers.

We also monitored the effect of Hsp90$_{Ec}$ on in vitro FtsZ assembly by light scattering (Fig. 4 *C* and *D*). Previous work demonstrated that there is a rapid increase in 90° light scattering following GTP addition to FtsZ that is caused by polymerization of FtsZ (Fig. 4*C*) (47). We observed that there was less light scattering when Hsp90$_{Ec}$ was incubated with FtsZ before the addition of GTP, compared with light scattering by FtsZ in the absence of Hsp90$_{Ec}$ (Fig. 4*C*). Moreover, as the concentration of
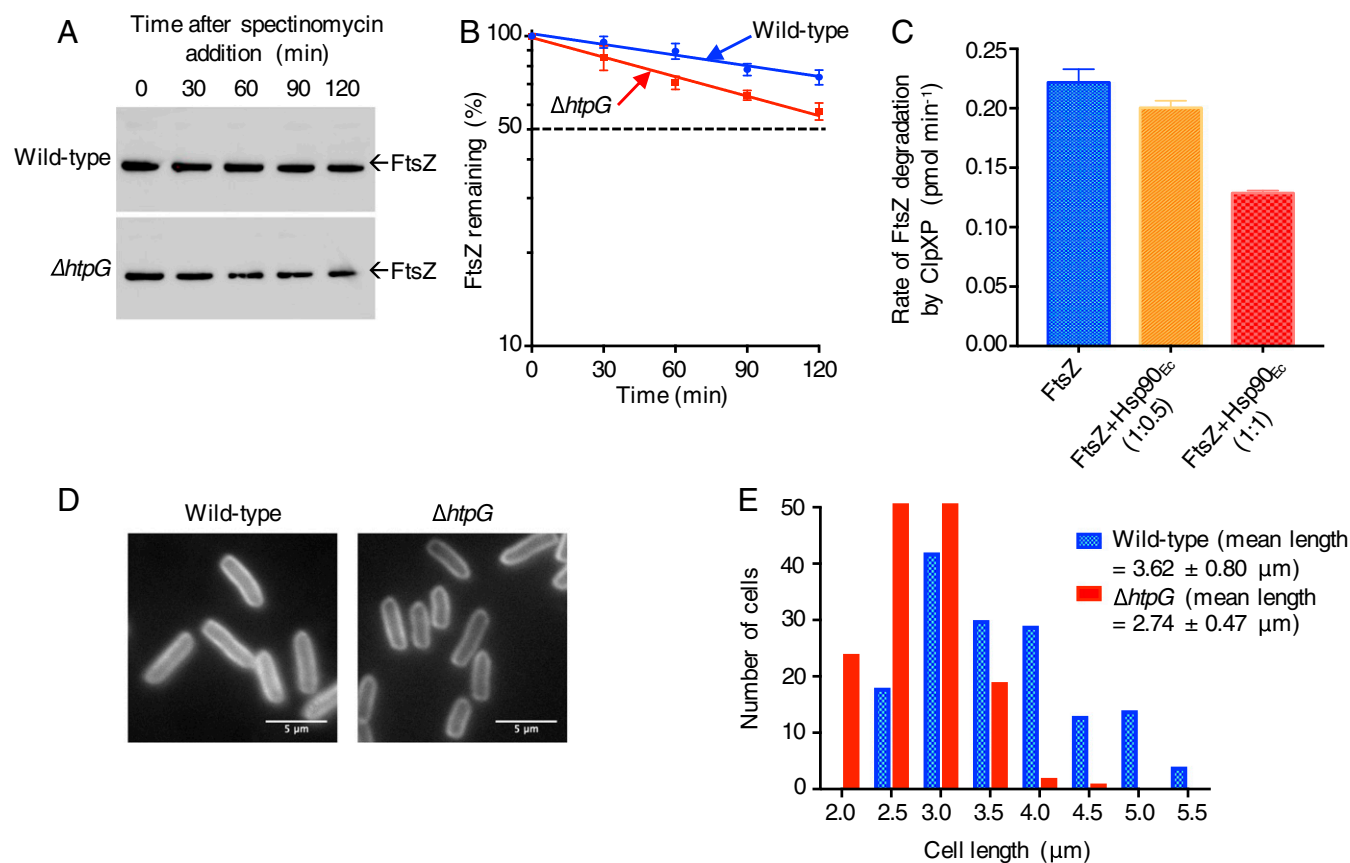
www.manaraa.com

Fig. 3. In cells lacking Hsp90$_{Ec}$, FtsZ is turned over more rapidly and cells are smaller. (*A*) Wild-type MG1655 and Δ*htpG* cultures were grown to an OD$_{600}$ of 0.6 and then 200 μg/mL spectinomycin was added. Samples were collected at the indicated times and analyzed by SDS/PAGE followed by immunoblotting with anti-FtsZ antibody as described in *Materials and Methods*. A representative experiment of four replicates is shown. (*B*) The rate of degradation of FtsZ in wild-type or Δ*htpG* cells was calculated from densitometric analysis of four independent immunoblots as shown in *A*. Data are presented as mean ± SD. The dashed line is 50% remaining, and meant to aid the eye. (*C*) In vitro degradation of FtsZ (10 μM) by ClpXP (1 μM) in the presence or absence of Hsp90$_{Ec}$ (5 or 10 μM) as described in *Materials and Methods*. Experiments were performed three times and data are presented as mean ± SD. (*D* and *E*) Wild-type MG1655 and Δ*htpG* cells were grown at 37 °C to an OD$_{600}$ of 0.6. (*D*) Cells were visualized by fluorescence microscopy following staining with FM 4-64 membrane stain as described in *Materials and Methods*. (Scale bars, 5 μm.) (*E*) Cell length was measured as described in *Materials and Methods* (150 each of wild type and Δ*htpG*). The cell-length distribution of wild-type and Δ*htpG* cells is shown and the mean length ± SD for each strain is indicated. In *D* and *E*, experiments shown are representative of three replicates.

Hsp90$_{Ec}$ was increased, the amount of light scattering observed decreased; when equimolar concentrations of FtsZ and Hsp90$_{Ec}$ were used, light scattering was reduced ~95%, compared with that observed in the absence of Hsp90$_{Ec}$ (Fig. 4*C*). Hsp90$_{Ec}$-E34A was also able to inhibit light scattering similar to wild type, indicating that ATP hydrolysis by Hsp90$_{Ec}$ was not required for prevention of FtsZ polymerization (Fig. 4*D*). These results show that Hsp90$_{Ec}$ inhibits FtsZ polymerization by an ATP-independent mechanism, supporting the fluorescence microscopy results.

The Hsp90$_{Ec}$ Client-Binding Region Is Involved in Interaction with FtsZ.
In previous work, we isolated Hsp90$_{Ec}$ mutants that blocked the Hsp90$_{Ec}$ overexpression phenotype of cell filamentation and showed that the mutants were defective in client binding by in vitro assays (Fig. 5*A*) (22). To determine if FtsZ interacted with the previously identified client-binding region of Hsp90$_{Ec}$, we tested several of the client-binding mutants for their ability to inhibit FtsZ polymerization as monitored by light scattering. Hsp90$_{Ec}$-W467R, the most defective client-binding mutant identified in the earlier study (22), was the most defective in preventing FtsZ assembly of the mutants tested (Fig. 5*B*). At a 1:0.5 FtsZ:Hsp90$_{Ec}$ ratio, Hsp90$_{Ec}$-W467R only decreased light scattering by ~13%, under conditions where wild-type Hsp90$_{Ec}$ decreased light scattering by ~74% (Fig. 5*B*). Two other client-binding mu-

tants, Hsp90$_{Ec}$-F554A and Hsp90$_{Ec}$-M546T, were partially defective in the ability to prevent FtsZ assembly, decreasing light scattering ~27 and ~39%, respectively (Fig. 5*B*). These results suggest that Hsp90$_{Ec}$ interacts with FtsZ specifically through its known client-binding region, and are consistent with the idea that Hsp90$_{Ec}$ overexpression leads to the cell-filamentation phenotype through FtsZ binding and sequestration.

The C-Terminal Tail of FtsZ Is Required for Interaction with Hsp90$_{Ec}$.
Previous work has demonstrated that many proteins that participate in cell division interact with residues in the C-terminal tail of FtsZ, including the membrane-tethering proteins FtsA and ZipA (48, 49) and the cell-division regulators ZapC, ZapD, SlmA, MinC, and ClpX (50–54). Additionally, the C-terminal tail is not required for polymerization of FtsZ (38). To test if Hsp90$_{Ec}$ also binds FtsZ via the C-terminal tail, we used fluorescence microscopy to visualize polymerization of an FtsZ variant with a C-terminal 18-amino acid truncation (44). FtsZΔ18 formed polymers in the presence but not the absence of GTP, as previously demonstrated (Fig. 6*A*, *1* and *2*) (44). In the presence of Hsp90$_{Ec}$, FtsZΔ18 polymerized as it did in the absence of Hsp90$_{Ec}$, suggesting Hsp90$_{Ec}$ was unable to interact efficiently with FtsZΔ18 (Fig. 6*A*, *3*).
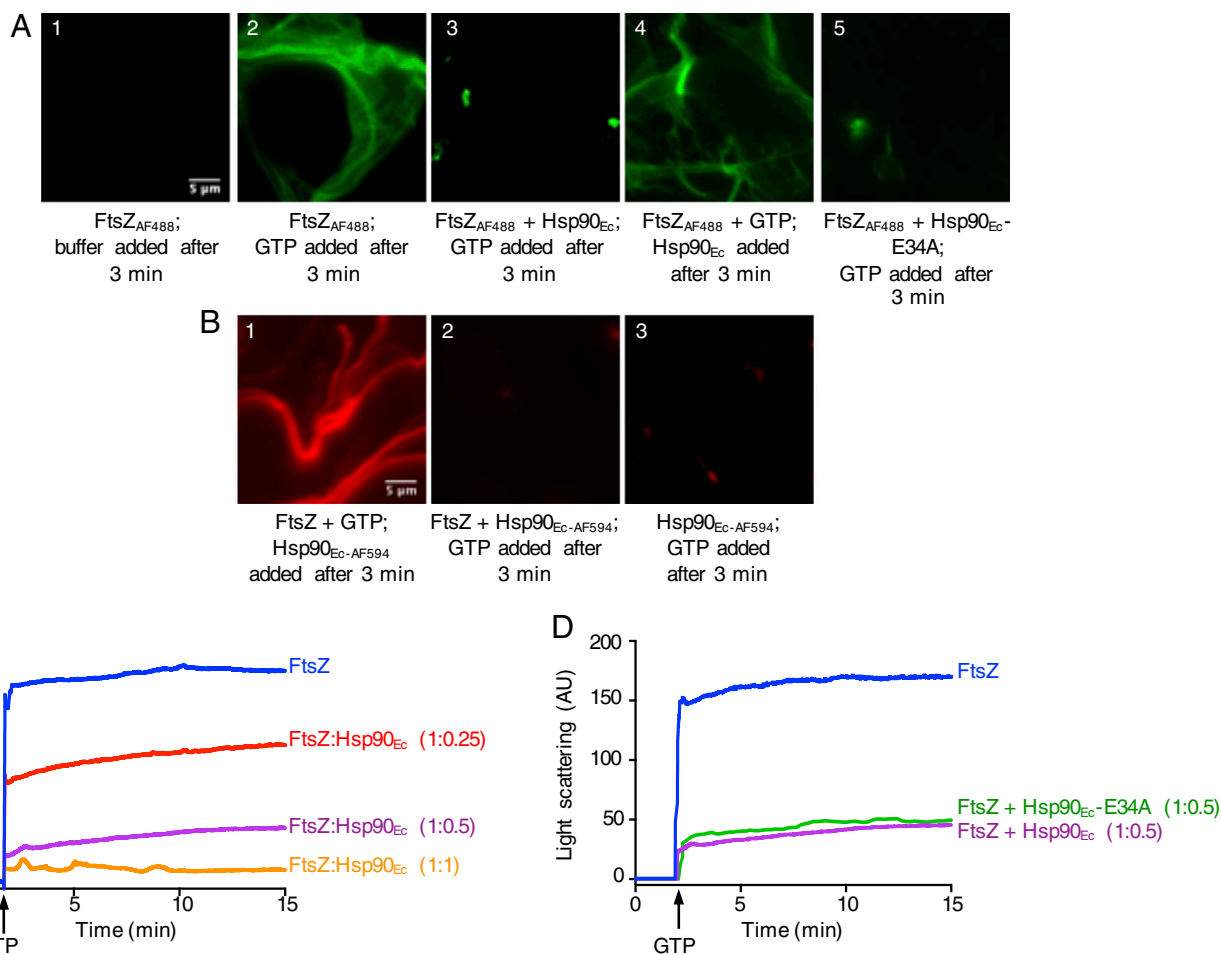
Fig. 4. $Hsp90_{Ec}$ inhibits assembly of FtsZ polymers in vitro. (*A* and *B*) Effect of $Hsp90_{Ec}$ on FtsZ polymerization as monitored by fluorescence microscopy. (*A*) Assays were carried out as described in *Materials and Methods* using 8 μM fluorescently labeled FtsZ ($FtsZ_{AF488}$) 4 μM $Hsp90_{Ec}$, or 4 μM $Hsp90_{Ec}$-E34A and 1 mM GTP as indicated. After incubation, samples were visualized by fluorescence microscopy. (*B*) FtsZ polymerization assays containing 4 μM fluorescently labeled $Hsp90_{Ec}$ ($Hsp90_{Ec-AF594}$) were performed as in *A* with 1 mM GTP and 8 μM FtsZ added as indicated. (Scale bars, 5 μm.) (*C* and *D*) FtsZ polymerization was monitored by 90° light scattering following the addition of GTP as described in *Materials and Methods*. (*C*) FtsZ (8 μM) was incubated in the absence or presence of 2, 4, or 8 μM $Hsp90_{Ec}$ for 2 min. GTP was then added (shown with a black arrow) and the reaction was allowed to continue. (*D*) FtsZ (8 μM) was incubated alone or with either 4 μM $Hsp90_{Ec}$ or 4 μM $Hsp90_{Ec}$-E34A for 2 min before GTP addition (shown with a black arrow). Representative results of three independent experiments are shown.

To verify a defect in interaction between an FtsZ C-terminal truncation mutant and $Hsp90_{Ec}$, we used 90° light scattering to monitor the assembly of full-length FtsZ or C-terminal truncation mutants FtsZΔ9 and FtsZΔ18 in the presence or absence of $Hsp90_{Ec}$. There was an immediate increase in light scattering when GTP was added to FtsZΔ9 and FtsZΔ18, similar to wild type, showing that the mutants were assembly-competent (Fig. 6*B*) (44, 50). When $Hsp90_{Ec}$ was incubated with either FtsZΔ9 or FtsZΔ18 before the addition of GTP, we observed an increase in light scattering similar to that seen in the absence of $Hsp90_{Ec}$, suggesting $Hsp90_{Ec}$ had no effect on polymerization of the truncated mutants (Fig. 6*B*). In comparison, $Hsp90_{Ec}$ inhibited light scattering by wild-type FtsZ by ∼70% (Fig. 6*B*). Together, these results show that residues in the C-terminal tail of FtsZ are important for the interaction between $Hsp90_{Ec}$ and FtsZ and for the inhibition of FtsZ polymerization by $Hsp90_{Ec}$. One interpretation is that by binding the FtsZ C-terminal tail, $Hsp90_{Ec}$ obstructs the FtsZ polymerization surface.

Discussion

Our results show that $Hsp90_{Ec}$, when expressed at high levels, inhibits cell division by blocking FtsZ-ring formation. Additionally,

purified $Hsp90_{Ec}$ interacts with FtsZ and inhibits FtsZ polymerization in vitro, in an ATP-independent reaction. Like many cell-division proteins and both positive and negative regulators of cell division, $Hsp90_{Ec}$ interacts with the C-terminal tail of FtsZ. Together, the results suggest that $Hsp90_{Ec}$ may modulate cell division by binding FtsZ and blocking FtsZ assembly and/or by competing with other FtsZ-interacting proteins to regulate FtsZ assembly and disassembly. They further suggest the possibility that *E. coli* Hsp90, and other Hsp90 proteins as well, may modulate important cellular processes by reversibly holding client proteins. Thus, the Hsp90 holdase activity could regulate the dynamic equilibrium between a free client protein and one bound to a functional partner, or it could modulate the equilibrium between various conformational states of a client protein.

Additional results presented here show that FtsZ is more stable in wild-type cells than in Δ*htpG* cells, suggesting that $Hsp90_{Ec}$ protects FtsZ from degradation. In vitro, we demonstrated that $Hsp90_{Ec}$ has the ability to inhibit degradation of FtsZ by ClpXP, a protease known to degrade *E. coli* FtsZ (44, 50). However, $Hsp90_{Ec}$ may also prevent other proteases from degrading FtsZ in vivo. Interestingly, previous work has suggested that $Hsp90_{Ec}$ can protect a number of clients from degradation.
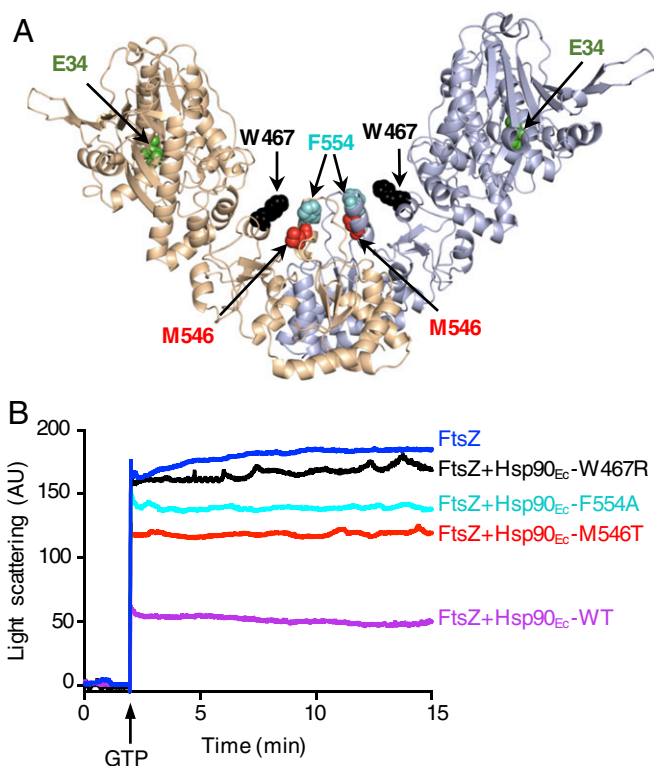
Fig. 5. Hsp90$_{Ec}$ mutants defective in client binding are defective in inhibiting FtsZ assembly in vitro. (*A*) Model of the Hsp90$_{Ec}$ dimer generated from the crystal structure of the apo form (PDB ID code 2IOQ) (64) and with the C-terminal domains aligned to the crystal structure of the isolated C-terminal domain (PDB ID code 1SF8) (65) using PyMOL (www.pymol.org). One monomer is colored wheat and the other is colored light blue. Client-binding residues, including W467, F554, and M546, are shown in black, cyan, and red, respectively, and the residue, E34, which is important for ATP hydrolysis, is shown in green; the mutated residues are represented as Corey–Pauling–Koltun models. (*B*) FtsZ polymerization after GTP addition was monitored by 90° light scattering as described in *Materials and Methods*. FtsZ (8 μM) was incubated alone or with 4 μM Hsp90$_{Ec}$ wild-type, W467R, F554A, or M546T, as indicated, for 2 min before GTP addition (shown with a black arrow). A representative experiment of three independent experiments is shown.

For example, extraintestinal pathogenic *E. coli* carrying a deletion of the gene encoding Hsp90$_{Ec}$ is nonvirulent and does not produce the genotoxin colibactin and the siderophore yersiniabactin (42). Virulence is restored if genes encoding the HslUV protease are also deleted, suggesting that Hsp90$_{Ec}$ protects a protein required for colibactin and yersiniabactin production from degradation (42). Additionally, CRISPR activity is defective in cells lacking Hsp90$_{Ec}$, and it has been shown that the defect is because an essential component of the CRISPR system, Cas3, is less stable in cells lacking Hsp90$_{Ec}$ than in wild-type cells (10). One speculation is that a general function of Hsp90 is to sequester unassembled polypeptides and protect them from cellular proteases.

Our results suggest that the client-binding and -holding function of Hsp90 may have physiological consequences that may be separate from its function as an ATP-dependent protein-remodeling machine. This ATP-independent activity may be a biologically important function of Hsp90 proteins in other organisms as well. The concept that Hsp90 may act to modulate the availability of specific cellular components as needed is similar to the buffering capacitor function of Hsp90 shown for higher eukaryotes. Eukaryotic Hsp90, by binding and stabilizing variant proteins, provides a storage facility that promotes evolution by releasing phenotypic variants when Hsp90 function is compromised under stressful conditions (55–57). Future work is required to test the generality

of the potential capacitor function of Hsp90 in modulating cellular processes.

Materials and Methods

Bacterial Strains and Plasmids. *E. coli* strains and plasmids used in this study are listed in *SI Appendix*, Table S1. Cells were grown in Luria–Bertani (LB) media supplemented with ampicillin (100 μg/mL), kanamycin (40 μg/mL), tetracycline (10 μg/mL), and chloramphenicol (25 μg/mL) as needed. *pgm* (JW0675), *clpX* (JW0428), *minC* (JW1165), *sulA* (JW0941), and *slmA* (JW5641) deletion mutants were acquired from the Keio collection (58) and introduced into MG1655 by P1 transduction (59). HC261(*zapA-gfp*) was a kind gift from Thomas G. Bernhardt, Harvard Medical School, Boston, MA (60). pZAQ plasmid was a kind gift from Joe Lutkenhaus, University of Kansas Medical Center, Kansas City, KS (61). To construct p$_{33}$Hsp90$_{Ec}$, pET-HtpG (16) was digested with XbaI and HindIII and the resulting fragment was ligated into similarly digested pBAD33. Frameshift mutations in pZAQ, including pZ*AQ, pZA*Q, and pZAQ*, were constructed as previously described (39). In experiments with p$_{33}$Hsp90$_{Ec}$ or its mutants, 0.2% arabinose was used for induction.

Proteins. Hsp90$_{Ec}$ wild type and mutants (16), FtsZ wild type and deletions (44), ClpX (62), and ClpP (63) were purified as previously described. Concentrations given are for Hsp90$_{Ec}$ dimer, FtsZ monomer, ClpX hexamer, and ClpP tetradecamer.

ZapA-GFP and Nucleoid Imaging. Cultures of MG1655 or HC261 carrying pHsp90$_{Ec}$ were grown at 37 °C in LB media overnight and diluted 1:50 into fresh medium, and 0.2% arabinose was added to induce Hsp90$_{Ec}$ expression. At various time points, cells were collected by centrifugation at 3,000 rpm for 10 min, resuspended in PBS, and placed on glass-bottom culture dishes
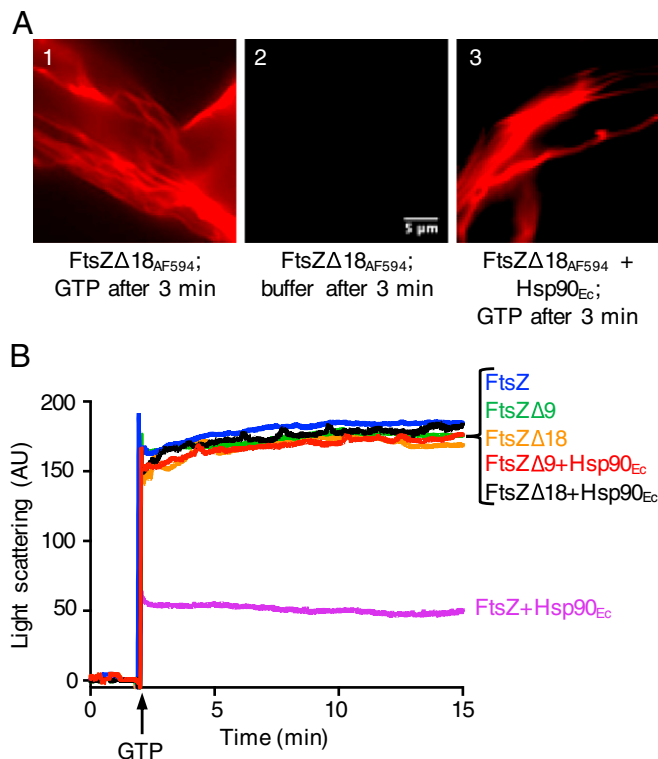

Fig. 6. FtsZ C-terminal tail is important for interaction with Hsp90$_{Ec}$. (*A*) Effect of Hsp90$_{Ec}$ on FtsZ polymerization was monitored by fluorescence microscopy as described in *Materials and Methods* using 8 μM FtsZΔ18, labeled with Alexa Fluor 594 (FtsZΔ18$_{AF594}$), 4 μM Hsp90$_{Ec}$, and 1 mM GTP where indicated and at the time indicated. After incubation, samples were visualized by fluorescence microscopy. (Scale bar, 5 μm.) (*B*) FtsZ polymerization was monitored by 90° light scattering following the addition of GTP as described in *Materials and Methods*. FtsZ, FtsZΔ9, or FtsZΔ18 (8 μM) was incubated for 2 min in the absence and presence of Hsp90$_{Ec}$ (4 μM) as indicated before GTP addition (shown with a black arrow). A representative experiment of three independent experiments is shown.

Balasubramanian et al.

www.manaraa.com

(MatTek). A 1% (wt/vol) agarose pad in PBS was placed on top of the cell suspension and cells were imaged with a DeltaVision (Applied Precision) IX71 microscope (Olympus), using a CoolSNAP HQ2 camera (Princeton Instruments) and a 300-W xenon light source through a 100× 1.40-numerical aperture oil-immersion objective. DIC images were acquired with an exposure time of 50 ms. For observing nucleoids, cells were stained with 1 μM Syto 9 (Thermo Fisher Scientific) for 15 min. ZapA-GFP and Syto 9 nucleoids were observed by fluorescence microscopy using the GFP/FITC filter set (ex 475/28 nm and em 525/50 nm) with exposure times of 2 s for ZapA-GFP and 25 ms for Syto 9-stained nucleoids, and photographed. Images were processed with NIH ImageJ software.

Determination of Cellular Levels of FtsZ by Immunoblotting. *E. coli* MG1655, carrying plasmids as indicated in the figure legends, were incubated with 0.2% arabinose. At the times indicated or after 4 h, 1-mL samples were removed, the cell density was determined (OD_{600}), the samples were precipitated with trichloroacetic acid (15% vol/vol) and centrifuged, and the resulting pellets were washed two times with 80% acetone. The pellets were resuspended in 100 μL of SDS/PAGE sample buffer. Sample volumes were normalized to cell density (OD_{600}) and subjected to SDS/PAGE, and the gels were analyzed by immunoblotting using anti-FtsZ antibody as previously described (44). FtsZ bands were quantified using NIH ImageJ software.

Cell-Length Measurements. *E. coli* MG1655 and MG1655 Δ*htpG* cells were grown in LB media at 37 °C to OD_{600} 0.6 or 1.2, as indicated. Cells (1 mL) were treated with 5 μg/mL FM 4-64 (Thermo Fisher Scientific) for 30 min in the dark to stain the outer membrane. Stained cells were washed twice with PBS and resuspended in PBS for microscopy.

Fluorescent images were acquired using a Zeiss 43HE (DsRed) filter set (ex 560/40 nm and em 630/75 nm) with an exposure time of 150 ms and photographed using an Axiocam camera connected to an Axio Imager M2 microscope (Zeiss) with an αPlan-Apochromat 100×/1.46-numerical aperture oil objective, and cell sizes were measured with AxioVision image analysis software.

Protein Turnover Experiments. *E. coli* MG1655 and MG1655 Δ*htpG* cells were grown in LB media at 37 °C to OD_{600} 0.6, and 200 μg/mL spectinomycin was added to inhibit protein synthesis. Samples (1 mL) were removed at the times indicated and processed as described above for the determination of cellular levels of FtsZ by immunoblotting.

FtsZ Polymerization Monitored by Light Scattering. FtsZ (8 μM) wild type or deletion mutant was incubated in FtsZ polymerization buffer (PB) (50 mM morpholino-ethanesulfonic acid, pH 6.5, 50 mM KCl, and 10 mM $MgCl_2$) with 25 μg/mL acetate kinase and 15 mM acetyl phosphate in a reaction volume of 200 μL with or without $Hsp90_{Ec}$ wild type or mutant (2, 4, or 8 μM) at 30 °C; 90° light scattering was monitored in a Cary Eclipse (Agilent) fluorescence spectrophotometer with excitation and emission wavelengths set to 400 nm with 5-nm slit widths. Baseline readings were collected for 2 min.

GTP (1 mM) was then added, and FtsZ polymerization was monitored for 15 min. Data were corrected for baseline readings.

FtsZ Polymerization Monitored by Fluorescence Microscopy. FtsZ wild type was labeled with NHS Alexa Fluor 488 (Thermo, Invitrogen) and FtsZΔ18 was labeled with NHS Alexa Fluor 594 (Thermo, Invitrogen) as described by the manufacturer. Reactions (50 μL) containing labeled FtsZ, $FtsZ_{AF488}$, or $FtsZΔ18_{AF594}$ (8 μM) were incubated with or without $Hsp90_{Ec}$ (4 μM) for 3 min at 30 °C in PB containing 25 μg/mL acetate kinase and 15 mM acetyl phosphate. GTP (1 mM) was then added and the reactions were incubated for an additional 3 min at 30 °C. Five microliters of the reaction was spotted on a slide, a coverslip was applied, and $FtsZ_{AF488}$ or $FtsZΔ18_{AF594}$ polymerization was assessed by fluorescence microscopy. Images were acquired using a Zeiss 38HE (eGFP) filter set (ex 470/40 nm and em 525/50 nm) for Alexa Fluor 488 and a Zeiss 43HE (DsRed) filter set (ex 560/40 nm and em 630/75 nm) for Alexa Fluor 594, with exposure time ranging from 20 to 100 ms. Images were photographed using an Axiocam camera connected to an Axio Imager M2 microscope (Zeiss) with an αPlan-Apochromat 100×/1.46-numerical aperture oil objective and processed with NIH ImageJ software. In some reactions, $Hsp90_{Ec}$ was added after the addition of GTP, as indicated, and FtsZ polymerization was monitored as described above.

To follow the localization of $Hsp90_{Ec}$ with FtsZ polymers, $Hsp90_{Ec}$ was labeled with NHS Alexa Fluor 594 (Thermo, Invitrogen) as described by the manufacturer. Polymerization reactions were carried out as described above using FtsZ wild type (8 μM) and $Hsp90_{Ec-AF594}$ (4 μM); $Hsp90_{Ec-AF594}$ localization was assessed by fluorescence microscopy. $Hsp90_{Ec-AF594}$ was also incubated in the absence of FtsZ and assessed by fluorescence microscopy as described above.

FtsZ Degradation Assays. FtsZ protein was labeled with NHS Alexa Fluor 488 (Thermo, Invitrogen) as described by the manufacturer, and $FtsZ_{AF488}$ degradation assays were carried out as previously described (50). Briefly, $FtsZ_{AF488}$ (10 μM) was incubated in the presence or absence of $Hsp90_{Ec}$ (5 or 10 μM) in PB at 30 °C for 5 min. ClpX (1 μM), ClpP (1 μM), and 4 mM ATP were added and incubated for 30 min at 30 °C. Reactions were stopped by the addition of 25 mM EDTA. Degradation products were isolated with Nanosep 10-kDa MWCO ultrafiltration devices (Pall), and prewashed with PB containing 0.01% Triton X-100. Eluent fluorescence was measured using a Tecan M200 Pro plate reader with excitation and emission wavelengths of 490 and 525 nm, respectively. $FtsZ_{AF488}$ processed as above in the absence of ClpXP was subtracted from the data.

1. L. H. Pearl, Review: The HSP90 molecular chaperone—An enigmatic ATPase. *Biopolymers* **105**, 594–607 (2016).
2. M. Radli, S. G. D. Rüdiger, Dancing with the diva: Hsp90-client interactions. *J. Mol. Biol.* **430**, 3029–3040 (2018).
3. F. H. Schopf, M. M. Biebl, J. Buchner, The HSP90 chaperone machinery. *Nat. Rev. Mol. Cell Biol.* **18**, 345–360 (2017).
4. J. C. Bardwell, E. A. Craig, Ancient heat shock gene is dispensable. *J. Bacteriol.* **170**, 2977–2983 (1988).
5. S. Lindquist, The heat-shock response. *Annu. Rev. Biochem.* **55**, 1151–1191 (1986).
6. J. G. Thomas, F. Baneyx, Roles of the *Escherichia coli* small heat shock proteins IbpA and IbpB in thermal stress management: Comparison with ClpA, ClpB, and HtpG in vivo. *J. Bacteriol.* **180**, 5165–5172 (1998).
7. J. G. Thomas, F. Baneyx, ClpB and HtpG facilitate de novo protein folding in stressed *Escherichia coli* cells. *Mol. Microbiol.* **36**, 1360–1370 (2000).
8. T. Inoue *et al.*, Genome-wide screening of genes required for swarming motility in *Escherichia coli* K-12. *J. Bacteriol.* **189**, 950–957 (2007).
9. A. M. Grudniak, K. Pawlak, K. Bartosik, K. I. Wolska, Physiological consequences of mutations in the htpG heat shock gene of *Escherichia coli*. *Mutat. Res.* **745–746**, 1–5 (2013).
10. I. Yosef, M. G. Goren, R. Kiro, R. Edgar, U. Qimron, High-temperature protein G is essential for activity of the *Escherichia coli* clustered regularly interspaced short palindromic repeats (CRISPR)/Cas system. *Proc. Natl. Acad. Sci. U.S.A.* **108**, 20136–20141 (2011).
11. O. Genest, S. Wickner, S. M. Doyle, Hsp90 and Hsp70 chaperones: Collaborators in protein remodeling. *J. Biol. Chem.* **294**, 2109–2120 (2019).
12. G. E. Karagöz, S. G. Rüdiger, Hsp90 interaction with clients. *Trends Biochem. Sci.* **40**, 117–125 (2015).
13. C. Prodromou, Mechanisms of Hsp90 regulation. *Biochem. J.* **473**, 2439–2452 (2016).
14. M. P. Mayer, L. Le Breton, Hsp90: Breaking the symmetry. *Mol. Cell* **58**, 8–20 (2015).
15. J. L. Johnson, Evolution and function of diverse Hsp90 homologs and cochaperone proteins. *Biochim. Biophys. Acta* **1823**, 607–613 (2012).
16. O. Genest, J. R. Hoskins, J. L. Camberg, S. M. Doyle, S. Wickner, Heat shock protein 90 from *Escherichia coli* collaborates with the DnaK chaperone system in client protein remodeling. *Proc. Natl. Acad. Sci. U.S.A.* **108**, 8206–8211 (2011).
17. S. Daturpalli, C. A. Waudby, S. Meehan, S. E. Jackson, Hsp90 inhibits α-synuclein aggregation by interacting with soluble oligomers. *J. Mol. Biol.* **425**, 4614–4628 (2013).
18. U. Jakob, H. Lilie, I. Meyer, J. Buchner, Transient interaction of Hsp90 with early unfolding intermediates of citrate synthase. Implications for heat shock in vivo. *J. Biol. Chem.* **270**, 7288–7294 (1995).
19. H. Nakamoto *et al.*, Physical interaction between bacterial heat shock protein (Hsp) 90 and Hsp70 chaperones mediates their cooperative action to refold denatured proteins. *J. Biol. Chem.* **289**, 6110–6119 (2014).
20. H. Wiech, J. Buchner, R. Zimmermann, U. Jakob, Hsp90 chaperones protein folding in vitro. *Nature* **358**, 169–170 (1992).
21. B. C. Freeman, R. I. Morimoto, The human cytosolic molecular chaperones hsp90, hsp70 (hsc70) and hdj-1 have distinct roles in recognition of a non-native protein and protein refolding. *EMBO J.* **15**, 2969–2979 (1996).
22. O. Genest *et al.*, Uncovering a region of heat shock protein 90 important for client binding in *E. coli* and chaperone function in yeast. *Mol. Cell* **49**, 464–473 (2013).
23. W. Margolin, FtsZ and the division of prokaryotic cells and organelles. *Nat. Rev. Mol. Cell Biol.* **6**, 862–871 (2005).
24. J. Lutkenhaus, S. Pichoff, S. Du, Bacterial cytokinesis: From Z ring to divisome. *Cytoskeleton (Hoboken)* **69**, 778–790 (2012).

Balasubramanian et al.

BIOCHEMISTRY

25. T. den Blaauwen, L. W. Hamoen, P. A. Levin, The divisome at 25: The road ahead. *Curr. Opin. Microbiol.* **36**, 85–94 (2017).

26. S. Du, J. Lutkenhaus, Assembly and activation of the *Escherichia coli* divisome. *Mol. Microbiol.* **105**, 177–187 (2017).

27. D. P. Haeusser, W. Margolin, Splitsville: Structural and functional insights into the dynamic bacterial Z ring. *Nat. Rev. Microbiol.* **14**, 305–319 (2016).

28. E. Nogales, K. H. Downing, L. A. Amos, J. Löwe, Tubulin and FtsZ form a distinct family of GTPases. *Nat. Struct. Biol.* **5**, 451–458 (1998).

29. J. Löwe, L. A. Amos, Evolution of cytomotive filaments: The cytoskeleton from prokaryotes to eukaryotes. *Int. J. Biochem. Cell Biol.* **41**, 323–329 (2009).

30. A. Mukherjee, J. Lutkenhaus, Guanine nucleotide-dependent assembly of FtsZ into filaments. *J. Bacteriol.* **176**, 2754–2758 (1994).

31. K. A. Michie, J. Löwe, Dynamic filaments of the bacterial cytoskeleton. *Annu. Rev. Biochem.* **75**, 467–492 (2006).

32. A. Mukherjee, J. Lutkenhaus, Dynamic assembly of FtsZ regulated by GTP hydrolysis. *EMBO J.* **17**, 462–469 (1998).

33. C. Ortiz, P. Natale, L. Cueto, M. Vicente, The keepers of the ring: Regulators of FtsZ assembly. *FEMS Microbiol. Rev.* **40**, 57–67 (2016).

34. D. W. Adams, J. Errington, Bacterial cell division: Assembly, maintenance and disassembly of the Z ring. *Nat. Rev. Microbiol.* **7**, 642–653 (2009).

35. V. W. Rowlett, W. Margolin, The Min system and other nucleoid-independent regulators of Z ring positioning. *Front. Microbiol.* **6**, 478 (2015).

36. N. W. Goehring, F. Gueiros-Filho, J. Beckwith, Premature targeting of a cell division protein to midcell allows dissection of divisome assembly in *Escherichia coli*. *Genes Dev.* **19**, 127–137 (2005).

37. F. J. Gueiros-Filho, R. Losick, A widely conserved bacterial cell division protein that promotes assembly of the tubulin-like protein FtsZ. *Genes Dev.* **16**, 2544–2556 (2002).

38. X. Ma, D. W. Ehrhardt, W. Margolin, Colocalization of cell division proteins FtsZ and FtsA to cytoskeletal structures in living *Escherichia coli* cells by using green fluorescent protein. *Proc. Natl. Acad. Sci. U.S.A.* **93**, 12998–13003 (1996).

39. K. Begg, Y. Nikolaichik, N. Crossland, W. D. Donachie, Roles of FtsA and FtsZ in activation of division sites. *J. Bacteriol.* **180**, 881–884 (1998).

40. J. E. Ward, Jr, J. Lutkenhaus, Overproduction of FtsZ induces minicell formation in *E. coli*. *Cell* **42**, 941–949 (1985).

41. M. Lu, N. Kleckner, Molecular cloning and characterization of the pgm gene encoding phosphoglucomutase of *Escherichia coli*. *J. Bacteriol.* **176**, 5847–5851 (1994).

42. C. Garcie *et al.*, The bacterial stress-responsive Hsp90 chaperone (HtpG) is required for the production of the genotoxin colibactin and the siderophore yersiniabactin in *Escherichia coli*. *J. Infect. Dis.* **214**, 916–924 (2016).

43. F. A. Honoré, V. Méjean, O. Genest, Hsp90 is essential under heat stress in the bacterium *Shewanella oneidensis*. *Cell Rep.* **19**, 680–687 (2017).

44. J. L. Camberg, J. R. Hoskins, S. Wickner, ClpXP protease degrades the cytoskeletal protein, FtsZ, and modulates FtsZ polymer dynamics. *Proc. Natl. Acad. Sci. U.S.A.* **106**, 10614–10619 (2009).

45. J. Lutkenhaus, S. G. Addinall, Bacterial cell division and the Z ring. *Annu. Rev. Biochem.* **66**, 93–116 (1997).

46. C. Graf, M. Stankiewicz, G. Kramer, M. P. Mayer, Spatially and kinetically resolved changes in the conformational dynamics of the Hsp90 chaperone machine. *EMBO J.* **28**, 602–613 (2009).

47. A. Mukherjee, J. Lutkenhaus, Analysis of FtsZ assembly by light scattering and determination of the role of divalent metal cations. *J. Bacteriol.* **181**, 823–832 (1999).

48. C. A. Hale, A. C. Rhee, P. A. de Boer, ZipA-induced bundling of FtsZ polymers mediated by an interaction between C-terminal domains. *J. Bacteriol.* **182**, 5153–5166 (2000).

49. X. Ma, W. Margolin, Genetic and functional analyses of the conserved C-terminal core domain of *Escherichia coli* FtsZ. *J. Bacteriol.* **181**, 7531–7544 (1999).

50. J. L. Camberg, M. G. Viola, L. Rea, J. R. Hoskins, S. Wickner, Location of dual sites in *E. coli* FtsZ important for degradation by ClpXP; one at the C-terminus and one in the disordered linker. *PLoS One* **9**, e94964 (2014).

51. S. Du, J. Lutkenhaus, SlmA antagonism of FtsZ assembly employs a two-pronged mechanism like MinCD. *PLoS Genet.* **10**, e1004460 (2014).

52. J. Durand-Heredia, E. Rivkin, G. Fan, J. Morales, A. Janakiraman, Identification of ZapD as a cell division factor that promotes the assembly of FtsZ in *Escherichia coli*. *J. Bacteriol.* **194**, 3189–3198 (2012).

53. C. Ortiz *et al.*, Crystal structure of the Z-ring associated cell division protein ZapC from *Escherichia coli*. *FEBS Lett.* **589**, 3822–3828 (2015).

54. B. Shen, J. Lutkenhaus, The conserved C-terminal tail of FtsZ is required for the septal localization and division inhibitory activity of MinC(C)/MinD. *Mol. Microbiol.* **72**, 410–424 (2009).

55. C. Queitsch, T. A. Sangster, S. Lindquist, Hsp90 as a capacitor of phenotypic variation. *Nature* **417**, 618–624 (2002).

56. N. Rohner *et al.*, Cryptic variation in morphological evolution: HSP90 as a capacitor for loss of eyes in cavefish. *Science* **342**, 1372–1375 (2013).

57. S. L. Rutherford, S. Lindquist, Hsp90 as a capacitor for morphological evolution. *Nature* **396**, 336–342 (1998).

58. Baba T, *et al.*, Construction of *Escherichia coli* K-12 in-frame, single-gene knockout mutants: The Keio collection. *Mol. Syst. Biol.* **2**, 2006 0008 (2006).

59. L. C. Thomason, N. Costantino, D. L. Court, *E. coli* genome manipulation by P1 transduction. *Curr. Protoc. Mol. Biol.* **79**, 1.17.1–1.17.8 (2007).

60. N. T. Peters, T. Dinh, T. G. Bernhardt, A fail-safe mechanism in the septal ring assembly pathway generated by the sequential recruitment of cell separation amidases and their activators. *J. Bacteriol.* **193**, 4973–4983 (2011).

61. E. Bi, J. Lutkenhaus, FtsZ regulates frequency of cell division in *Escherichia coli*. *J. Bacteriol.* **172**, 2765–2768 (1990).

62. R. Kruklitis, D. J. Welty, H. Nakai, ClpX protein of *Escherichia coli* activates bacteriophage Mu transposase in the strand transfer complex for initiation of Mu DNA synthesis. *EMBO J.* **15**, 935–944 (1996).

63. M. R. Maurizi, M. W. Thompson, S. K. Singh, S. H. Kim, Endopeptidase Clp: ATP-dependent Clp protease from *Escherichia coli*. *Methods Enzymol.* **244**, 314–331 (1994).

64. A. K. Shiau, S. F. Harris, D. R. Southworth, D. A. Agard, Structural analysis of *E. coli* hsp90 reveals dramatic nucleotide-dependent conformational rearrangements. *Cell* **127**, 329–340 (2006).

65. S. F. Harris, A. K. Shiau, D. A. Agard, The crystal structure of the carboxy-terminal dimerization domain of htpG, the *Escherichia coli* Hsp90, reveals a potential substrate binding site. *Structure* **12**, 1087–1097 (2004).

www.manaraa.com